Damage detection and characterization using EMI technique under varying axial load

Lim, Yee Yan; Soh, Chee Kiong

2013

Lim, Y. Y., & Soh, C. K. (2013). Damage detction and characterization using EMI technique under varying axial load. Smart structures and systems, 11(4), 349-364.

https://hdl.handle.net/10356/103996

https://doi.org/10.12989/sss.2013.11.4.349

DAMAGE DETECTION AND CHARACTERIZATION USING EMI TECHNIQUE UNDER VARYING AXIAL LOAD

YEE YAN LIM*[1a] AND CHEE KIONG SOH[2b]

[1] *Civil Engineering Program, School of Engineering & Information Technology, University Malaysia Sabah, Locked Bag No. 2073, 88999 Kota Kinabalu, Sabah, Malaysia.*

[2]*Division of Structures and Mechanics, School of Civil and Environmental Engineering, Nanyang Technological University, 50 Nanyang Avenue, Singapore 639798.*

Abstract. Recently, researchers in the field of structural health monitoring (SHM) have been rigorously striving to replace the conventional NDE techniques with the smart material based SHM techniques, employing smart materials such as piezoelectric materials. For instance, the electromechanical impedance (EMI) technique employing piezo-impedance (lead zirconate titanate, PZT) transducer is known for its sensitivity in detecting local damage. For practical applications, various external factors such as fluctuations of temperature and loading, affecting the effectiveness of the EMI technique ought to be understood and compensated. This paper aims at investigating the damage monitoring capability of EMI technique in the presence of axial stress with fixed boundary condition. A compensation technique using effective frequency shift (EFS) by cross-correlation analysis was incorporated to compensate the effect of loading and boundary stiffening. Experimental tests were conducted by inducing damages on lab-sized aluminium beams in the presence of tensile and compressive forces. Two types of damages, crack propagation and bolts loosening were simulated. With EFS for compensation, both cross-correlation coefficient (CC) index and reduction in peak frequency

were found to be efficient in characterizing damages in the presence of varying axial loading.

Keywords: Electromechanical impedance (EMI), piezoceramics (PZT), axial load, structural health monitoring (SHM), smart materials, effective frequency shift (EFS), cross-correlation coefficient (CC)

* Corresponding author

[a] Lecturer, *yylim@ums.edu.my*

[b] Professor, *csohck@ntu.edu.sg, (65) 6790-5280*

1. Introduction

Continuous SHM is essential to ensure timely repair and maintenance, in order to preserve the integrity and serviceability of the structure at minimum cost. In the case of potential structural failure, early warning can minimize human and property losses.

Non-destructive evaluation (NDE) techniques such as ultrasonic wave propagation, acoustic emission, magnetic field analysis, dye penetration test, eddy currents and X-ray radiography are commonly used in the industry for damage detection. However, these techniques generally depend heavily on visual inspection for gross assessment prior to applying the local techniques to pinpoint the damage. These conventional techniques can sometimes be inefficient and tedious. In large structures, the critical parts may not be readily accessible. This situation is further aggravated by the requirement of bulky probes or equipment to be carried along during inspection. Inspectors can also be exposed to dangerous conditions or uncomfortable working environments. High dependency of visual inspection on experience of the inspector, high cost and unsystematic procedures render the technique uneconomical and unreliable.

Recently, researchers in the field of SHM have been rigorously striving to replace the conventional NDE techniques with the smart material based SHM techniques, employing smart materials such as piezoelectric materials and fiber optics. These techniques possess distinct advantages over the conventional techniques, such as capable of providing autonomous, real-time, reliable and cost efficient monitoring. One of these techniques, known as the electromechanical impedance (EMI) technique employing smart piezo-impedance (lead zirconate titanate, PZT) transducer is known for its sensitivity in detecting local damage.

Being non-invasive, extremely light, cost effective, able to perform self-actuating and self-sensing, the EMI technique is constantly being developed in recent decades.

For instance, Ayres et al. (1998) studied qualitatively the feasibility of employing the EMI technique on a quarter-scale deck truss bridge joint. Park et al. (2000) reported significant proof-of-concept applications of the EMI technique on civil-structural components such as composite reinforced masonry walls, steel bridge joints and pipe joints. Soh et al. (2000) established the damage detection and localization ability of piezo-impedance transducers on real-life RC structures. Lim et al. (2006) attempted some parametric based damage detection using equivalent structural parameters in characterizing the severity of damage in lab-sized aluminium and concrete structure. Lim and Soh (2011) developed a proof-of-concept damage prognosis model useful for estimating the remaining useful life of fatigue loaded 1-D structure.

Park et al. (2008a) adopted the PCA-data compression technique as a pre-processing module to reduce the data dimensionality and eliminate the unwanted noises, which is useful for wireless monitoring. Experimental study inspecting loose bolts in a bolt-jointed aluminium structure was conducted. The damage detection capability is significantly enhanced in comparison to the traditional root mean square deviation approach. Min et al. (2010) proposed an innovative technique for autonomous selection of damage-sensitive frequency ranges using artificial neural networks.

The EMI technique is also able to monitor the hydration process of concrete. For instance, Shin et al. (2008) showed that the EMI signatures obtained from PZT patch surface bonded on concrete gradually shifted to the right and subsided with curing time. They

attributed these behaviors to the stiffening action due to strength gain of concrete.

For practical applications, various issues ought to be overcome. For instance, large numbers of sensors are required to monitor a large structure which poses problems such as wiring. One way of overcoming the hassle of wires is to employ the wireless technology. However, active sensing device such as PZT transducer would normally require relatively high electrical power. Battery replacement of remotely placed sensors could be extremely tedious if not impossible.

Alternate power supply such as through Radio Frequency (RF) microwave transmission to wirelessly transmit power to an active sensor node is a possibility. The RF microwaves can be transmitted through the atmosphere to a receiver to be converted into DC power (Mascarenas et al. 2007). A self-contained wireless sensor incorporating various functions including on-board actuating/sensing, power generation, on-board data processing/damage diagnostic and RF module is continuously being pursued by researchers such as Inman and Grisso (2006) and Park et al. (2006).

Additionally, fluctuations of temperature (Yang et al. 2008) and loading can also affect the effectiveness of EMI in SHM. Compensation techniques to tackle the fluctuation of temperature have been presented by Park et al. (1999) and Koo et al. (2009). Detailed reviews considering various issues on the applications of EMI technique in SHM can be obtained in publications by Park et al. (2003, 2008b) and Annamdas and Soh (2010).

Yang and Miao (2010) have conducted experimental and analytical investigations into the effect of ambient vibration using aluminium beam. They concluded that the effect of external vibration on PZT signatures could not be ignored when the external excitation

frequency and PZT's actuation frequency are comparable (2/5 < external frequency / PZT frequency < 10). In general, the effect of ambient vibration (typically < 100 Hz) would not affect the admittance signatures (typically > 10 kHz) significantly.

Up to date, there are only a few studies (Annamdas et al. 2007, Abe et al. 2000, Ong et al. 2002, Lim and Soh, 2012) conducted to investigate the effect of static axial load on admittance signatures. The damage detection capability of EMI technique in the presence of varying axial load has yet to be investigated.

This paper aims at investigating the feasibility of EMI technique in damage monitoring in the presence of axial stress with fixed boundary condition. A compensation technique using effective frequency shift (EFS) by cross-correlation analysis was incorporated to compensate the effect of loading and boundary stiffening. Experimental tests were conducted by inducing different damages on lab-sized aluminium beams in the presence of tensile and compressive forces. Damage detection capability of EMI technique under varying compressive force was investigated.

2. EMI technique for SHM

The EMI technique shares similar working principles as the conventional global dynamic response techniques. However, the frequency range employed (30 - 1000 kHz) is much higher. The method of interrogation also differs. The use of high frequency of excitation renders the EMI technique to be very effective in detecting local damage, even in its incipient stage.

In the application of EMI technique, a mechanically attached (surface-bonded or embedded) PZT patch is dynamically excited by an alternating (sinusoidal) voltage, sourced

by an impedance analyzer, uniformly across the patch. The vibrational force generated by the PZT patch can then be transferred to the host structure. The corresponding structural response at different excitation frequency will modulate the electric current across the PZT patch.

The modulated current, in terms of complex electrical admittance (conductance and susceptance signatures) is also measured and recorded by the impedance analyzer at predetermined frequency interval. Any subsequent damage or interference on the structure, which causes a change in structural response, can be reflected from the alteration in the spectrum. According to the structural dynamic theory, the occurrence of damage would reduce the overall structural stiffness which can generally be reflected through the reduction in modal frequency.

Liang et al. (1994) introduced a 1-D EMI model by simplifying the PZT patch into a thin bar undergoing axial vibrations. Its interaction with the host structure is confined to the end points, as illustrated in Fig. 1. Assuming perfect bonding between the PZT patch and the host structure, the entire structure is represented by its driving point mechanical impedance. Incorporating the dynamic force equilibrium and the piezoelectric constitutive relations, Liang et al. (1994) derived the following expression for the electro-mechanical admittance based on 1-D modeling:

$$\overline{Y} = 2\omega j \frac{w_a l_a}{h_a}\left[\overline{\varepsilon_{33}^{T}} + \left(\frac{Z_a}{Z+Z_a}\right) d_{31}^2 \overline{Y_{11}^{E}} \left(\frac{\tan \kappa l_a}{\kappa l_a}\right) - d_{31}^2 \overline{Y_{11}^{E}}\right] \qquad (1)$$

where ω is the angular frequency of the driving voltage, j is the imaginary number, and w_a, l_a and h_a are the width, length and thickness of the PZT patch respectively. $\overline{Y_{11}^{E}}$ is the complex Young's modulus, $\overline{\varepsilon_{33}^{T}}$ is the complex electric permittivity, d_{31} is the piezoelectric strain coefficient and κ is the wave number. Z_a and Z are the mechanical impedance of the PZT

patch and the structure respectively. According to the impedance approach, the mechanical impedance of the PZT patch, Z_a can be derived as:

$$Z_a = \frac{\kappa w_a h_a \overline{Y_{11}^E}}{(j\omega)\tan(\kappa l_a)} \tag{2}$$

In general, the local damage detection capability of the EMI technique has been well accepted. Damage characterization is often achieved through statistical quantifiers. Advantages can be seen from the fact that no information regarding the structure is required in advance. Root mean square deviation (RMSD) and cross-correlation coefficient (CC) are among the commonly used non-parametric quantification approaches.

In this study, the damage detection capability of EMI technique under varying axial load was experimentally investigated. This study is important because a structure in service is inevitably loaded by at least its self-weight and dead load. The effect of loading on the admittance signatures acquired cannot be ignored for an efficient SHM.

Annamdas et al. (2007) showed that the electrical admittance signatures, especially its imaginary component adopted in the EMI technique is susceptible to variation upon the application of static load on the host structure. On the other hand, applied loads are associated with the imposed boundary conditions. Annamdas and Soh (2010) reported in a review paper that if the host structure is smaller than the sensing range of the PZT transducer bonded on it, the boundary conditions can also influence the PZT-based signatures. Park et al. (2000) claimed that the sensing radius of a typical PZT patch might vary from 0.4m on composite reinforced structures to about 3m on simple metal beams. The boundary conditions in real life structures are however, extremely difficult to characterize analytically, and tend to exhibit poor repeatability between structures (David, 2006).

Abe et al. (2000) first proposed the use of EMI technique for identification of in-situ stress in thin structural members. Both 1-D and 2-D analytical models based on wave propagation theory for beam and plate structures were developed, incorporating the effect of axial stress. They showed that the tensile stress increased the resonance frequency in the electrical impedance spectrum. However, they found that considerable discrepancy existed between the measured and the predicted stress. No in-depth reasoning was provided regarding the difference.

Ong et al. (2002) investigated the effect of in-situ stress on the frequency response function (FRF) of beam structure by applying pure bending actuation through a pair of symmetrically located surface-bonded PZT transducers, activated in out-of phase mode. They simulated the axially loaded beam structure with PZT patch using 1-D EMI model for an elastically constrained transducer. Back calculation of the in-situ stress from the electrical FRF of the transducer was presented. However, experimental verification was not included.

Lim and Soh (2012) performed a series of studies involving analytical and numerical modeling as well as experimental test to investigate the effect of axial stress on admittance signatures under fixed boundary condition. Discrepancies between theory and experiment were attributed to the stiffening effect caused by the boundary condition. The effect of boundary condition was found to be more dominant in comparison to the axial stress.

In this study, the effective frequency shift (EFS) through cross-correlation analysis for compensating the effect of temperature proposed by Koo et al. (2009) was utilized to compensate the effect of static axial stress. The EFS, $\tilde{\omega}$ for an impedance data $y(\omega)$ is defined as the shift corresponding to the maximum CC (as closed to unity as possible) with

the reference impedance data $x(\omega)$, which can be expressed as:

$$\max CC(\tilde{\omega}) = \max\left\{\frac{\frac{1}{N}\sum_{i=1}^{N}\left[x_i(\omega_i)-\bar{x}\right]\left[y_i(\omega_i-\tilde{\omega})-\bar{y}\right]}{\sigma_x\sigma_y}\right\} \quad (3)$$

where $y_i(\omega_i)$ is the impedance data of interest, $x_i(\omega_i)$ is the reference impedance data measured at i^{th} frequency, σ_x, σ_y and $\bar{x}$, $\bar{y}$ are the standard deviations and means of data x and data y respectively.

3. Experimental Setup and Test

Three aluminium (grade Al6061-T6) beam specimens of size 231mm x 26mm x 4mm were prepared in this experiment. One piece of PZT patch (type PIC 151, manufactured by PI Ceramics) measured 10mm x 10mm x 0.3mm was surface-bonded on each of the specimen using two parts high strength epoxy. The configurations of the specimens, the damage induced and the loading applied are summarized in Table 1 and depicted in Fig. 2.

In the experiment, tensile force was applied on specimen T1 using a Universal Test Machine (UTM) as shown in Fig. 3(a). Specimens C1 and C2 were loaded on a strut rig (TQ SM 105 Mk II) as illustrated in Fig. 3(b).

Wayne Kerr precision impedance analyzer 6420 (Fig. 3c) was used to supply alternating voltage and to measure the corresponding admittance signatures across the PZT patch. A notebook computer with customized software was used to record the admittance signatures.

3.1 Repeatability of admittance signatures under varying axial load

In the application of EMI technique, a set of baseline signatures at the healthy stage is

always required to compare with the subsequent signatures, carrying information of damages. In this case, multiple baseline signatures at different loadings are required. A set of baseline signatures of a particular load is then selected as reference, in which all other sets will be compensated against it. In this study, only the conductance (real component of admittance) signatures were utilized as the real part is generally more sensitive to damages (Sun et al. 1995).

Before inducing any damages, it is important to confirm the repeatability of the admittance signatures under constant and varying stresses. Firstly, several sets of signatures were acquired with 3kN of tensile load applied. Consistency was maintained as long as the boundary condition was not disturbed, as shown in Fig. 4(a), where the peak frequencies, slopes and amplitudes of the signatures taken from two different readings were matching each other almost exactly. The CC value from 10 ~ 100 kHz was calculated to be 0.97, implying that both signatures match each other almost exactly.

A similar test was conducted on specimen C1 subjected to 1000N of compression force. In this case, a set of signatures was first acquired after the load was increased from 0 to 1000N. Then, another set of signatures was recorded after the load was further increased to 1200N and released back to 1000N. The conductance plot is shown in Fig. 4(b). Repeatability remains high in spite of the process of loading and unloading, as long as the boundary condition is maintained.

4. Damage monitoring of EMI technique in presence of axial load

4.1 Crack detection under constant tensile load

After confirming their repeatability, the damage detection capability of EMI technique under constant tensile force was investigated. A crack was progressively induced, using a handsaw, from 1mm to 9mm on specimen T1 with the tensile load maintained at 3kN. The thickness of the saw tooth was approximately 0.5mm. The sawing process was conducted with care to prevent intervention to the boundary condition. The fluctuation of load during the sawing process was observed to be less than 0.08kN.

Fig. 5 presents the CC indices evaluated in three frequency ranges, 10 ~ 20 kHz, 40 ~ 50 kHz and 90 ~ 100 kHz. The CC indices decreased progressively as the damage, in terms of crack length, became more severe. Generally, the higher frequency range (80 ~ 90 kHz) is more sensitive to small crack (especially when crack is less than 3mm). The lower frequency range (10 ~ 20 kHz) is however, more consistent in characterizing larger crack (5mm or more).

Referring to the conductance signature plot shown in Fig. 6, the resonance peak's frequency reduced progressively with damage. In the lower frequency range (19.4 ~ 20.4 kHz) as shown in Fig. 6(a), the resonance peak shift progressively to the left with increase in crack length. This frequency range is relatively less sensitive to smaller crack (less than 3mm) as compared to the higher range (81.7 ~ 83.7 kHz) as shown in Fig. 6(b). In the higher range, crack as small as 1mm can be characterized. However, the higher range can be less effective when the damage is relatively severe. For instance, upon induction of a 7mm crack, the peak in the higher range completely disappeared, implying a severe alteration in vibrational behavior. On the other hand, peak movement up to 9mm crack can be clearly observed in the lower range. Higher sensitivity of the higher frequency range could be easily explained by the

fact that the wavelength in the higher range is smaller than the lower range, allowing interaction with smaller crack.

The conductance plot reflects the physical meaning of the CC indices. Physically, the reduction in resonance frequency can be explained by the fact that damage reduces the stiffness of the structure, inducing a leftward shift in electromechanical resonance peak, representative of the structural vibrational behavior.

In actual application, one should always refer to the conductance signatures for more physical insight instead of relying merely on the damage indices, which can sometimes be inconsistent.

4.2 Crack detection under varying compressive load

The above study proves that the EMI technique is effective for damage detection under constant tensile load. Next, the effect of varying axial stress which included the effect of boundary stiffening was considered. In the presence of varying compressive axial load with fixed boundary condition, a propagating crack was induced on specimen C1 (Fig. 2a). Three baseline signatures at 900N, 1000N and 1100N were taken.

Similar to the previous test, a progressively sever crack, from 1mm to 9mm was induced. For each crack length, the admittance signatures were acquired under the abovementioned three different compressive loads.

The experimental tests conducted in this study showed that increase in loading will induce a rightward shift in resonance peak, implying a stiffening effect as shown in Fig. 7(a). For tensile force, rightward shift of peak was caused by stiffening of host structure. For

compressive force, rightward shift of peak was mainly caused by stiffening of boundary condition (Lim and Soh, 2012). No vertical shift was observed.

In order to compensate the effect of axial load, EFS using CC was performed by adopting the signatures acquired at 900N as baseline. A computer program capable of automatically performing the compensation for a selected frequency of different loading was developed in Matlab language based on Eq. (3). The program enables the load and frequency of interest to be entered, after which the EFS will be evaluated based on the maximum CC value. Fig. 7 illustrates the signatures in the range of 45.4 to 47 kHz for all three loading before and after compensation. Obviously, the resonance peak matches each other closely after compensation. Since the movements in resonance peaks can differ among different frequency range, selection of range for compensation shall be kept narrow.

Next, the same peak from Fig. 7 containing damaged information were considered and summarized graphically in Fig. 8. Fig. 8(a) and (b) compare the peak frequencies whereas Fig. 8(c) and (d) compare the CC values before and after performing the compensation, respectively. Note that the EFS compensations performed at the healthy stage are applicable to the damaged state.

Fig. 8(b) and (d) clearly indicate that upon compensation, the damage characterization capability of EMI technique remains effective in spite of the presence of fluctuating load. Compensation is especially important for the CC damage index, without which could lead to false alarm as shown in Fig. 8(c). The CC values, upon compensation, once again correlate well with the crack length and agree closely with the frequency reduction. Other frequency ranges can similarly be used which exhibit similar behavior as specimen T1, which is herein

omitted.

4.3 Detection of bolt loosening under varying compressive load

Besides crack, several other forms of damage could occur in a structure. Another experimental test was conducted to monitor the loosening of bolts on specimen C2 under different compressive axial load using the EMI technique. Three holes of 5mm diameter were created in specimen C2. Three sets of identical bolts (5mm diameter) and nuts were tightened by hand through the holes as shown in Fig. 2(b). Damage was simulated by loosening the nuts (360^0 turn), one at a time starting from the bolt furthest away from the PZT patch, labeled as bolt C. After acquiring the signatures, bolt B was loosened. Finally, bolt A was loosened. For the sake of presentation, we classified each stage of damage into damage levels as tabulated in Table 2.

Fig. 9 illustrates the conductance signatures with different damage levels in the frequency range of 40 to 80 kHz under 900N of compression. In this case, the changes in admittance signatures were more erratic. Identification of peak's movement was impossible because several peaks disappeared and new peaks emerged after each stage of damage. This phenomenon is conceivable because loosening one bolt is equivalent to creating a 5mm hole, which can be considered as a severe damage relative to the size of the beam.

Therefore, only the CC damage index was used for characterizing the crack. The CC values, upon compensating with respect to 900N of load are presented in Fig. 10. A wider frequency range from 40 ~ 80 kHz was adopted. The CC index decreased progressively as the number of loosened bolts increased. The CC index acquired from damage level 3 and level 4

were identical. This implies that upon loosening all the bolts, the extent of damage was equivalent to no bolt. Referring to the conductance plot in Fig. 9, damage level 3 and level 4 are basically overlapping each other, confirming the outcome of the CC index.

Both of the studies presented above concentrated on the damage detection and characterization of the EMI technique under varying static axial load in the presence of fixed boundary conditions. Both sets of results indicate that the EMI technique remains efficient in damage monitoring upon EFS compensation. In real-life applications, various data normalization technique can also be used to compensate these effects, such as artificial neural network (ANN), linear principal component analysis (LPCA) and Kernel principal component analysis (KPCA). The effect of temperature can also be included. For large amount of data, outlier analysis can be performed for damage detection with statistical confidence (Koo et al., 2009).

5. Conclusions

This paper presents a series of experimental investigations to study the feasibility of damage detection and characterization using the EMI technique in the presence of varying load with fixed boundary conditions. EFS using maximum CC was adopted for compensating the effect of axial load, which caused predominantly horizontal shift. Both tensile and compressive forces were considered. Two types of damages, crack propagation and bolts loosening were simulated. With EFS for compensation, both CC index and reduction in peak frequency are efficient in characterizing the damages in the presence of axial loading. Further study may focus on experimental test on large-scale structures before real-life application is

possible.

References

Abe, M., Park, G. and Inman, D. J. (2002), "Impedance-based monitoring of stress in thin structural members", *Proceeding of 11th International Conference on Adaptive Structures and Technologies*, October 23-26, Nagoya, Japan, 285-292.

Annamdas, V. G. M. and Soh, C. K. (2007), "Three dimensional electromechanical impedance model I: Formulation of directional sum impedance", *Journal of Aerospace Engineering*, American Society of Civil Engineers, **20**(1), 53-62.

Annamdas, V. G. M. and Soh, C. K. (2010), "Application of electromechanical impedance technique for engineering structures: Review and future issues", *Journal of Intelligent Material Systems and Structures*, **21**(1), 41-59.

Ayres, J. W., Lalande, F., Chaudhry, Z. and Rogers, C. A. (1998), "Qualitative Impedance-Based Health Monitoring of Civil Infrastructures", *Smart Materials and Structures*, **7**(5), 599-605.

David, D. L. M. (2006), "Development of an impedance method based wireless sensor node for monitoring of bolted joint preload", *Master of Science Dissertation*, University of California, San Diego, USA.

Inman, D. J. and Grisso, B. L. (2006), "Towards autonomous sensing", *Proceedings of SPIE International Conference on Smart Structures and Materials*, February 26-March 2, San Diego, CA, **6174**, 248-254.

Koo, K.-Y., Park, S., Lee, J.-J. and Yun, C.-B. (2009), "Automated impedance-based structural health monitoring incorporating effective frequency shift for compensating temperature effects", *Journal of Intelligent Material Systems and Structures*, **20**, 367-377.

Liang, C., Sun, F. P. and Rogers, C. A. (1994), "Coupled electro-mechanical analysis of adaptive material systems - determination of actuator power consumption and system energy transfer", *Journal of Intelligent Material Systems and Structures*, **5**, 12-20.

Lim, Y. Y., Bhalla, S. and Soh, C. K. (2006), "Structural identification and damage diagnosis using self-sensing piezo-impedance transducers" *Smart Mater. Struct.*, **15**, 987-95.

Lim, Y. Y., and Soh, C. K. (2011) "Fatigue life estimation of a 1D aluminium beam under mode-I loading using the electromechanical impedance technique", *Smart Mater. Struct.*, **20**, 125001.

Lim, Y. Y., and Soh, C. K. (2012) "Effect of varying axial load under fixed boundary condition on admittance signatures of electromechanical impedance Technique", *Journal of Intelligent Material Systems and Structures*, **23**(7), 815-826.

Mascarenas, D. L., Todd, M. D., Park, G., and Farrar, C. R. (2007), "Development of an impedance-based wireless sensor node for structural health monitoring", *Smart Mater. Struct.*, **16**(6), 2137-2145.

Min, J., Park, S. and Yun, C.-B. (2010), "Impedance-based structural health monitoring using neural networks for autonomous frequency range selection", *Smart Mater. Struct.*, **19** 125011

Ong, C.W., Yang, Y., Naidu, A.S.K., Lu, Y., Soh, C.K. (2002), "Application of the electromechanical impedance method for the identification of in-situ stress in structures," *Proceedings of SPIE on Smart Structures, Devices and Systems*, December 16-18, Melbourne, 503-514.

Park, G., Cudney, H. H. and Inman, D. J. (2000), "Impedance-based health monitoring of civil structural components", *Journal of Infrastructure Systems*, ASCE, **6**(4), 153-160.

Park, G., Kabeya, K., Cudney, H. H. and Inman, D. J. (1999), "Impedance-based structural health monitoring for temperature varying applications", *JSME International Journal*, **42**(2), 249-258.

Park, S., Lee, J. J., Inman, D. J. and Yun, C. - B. (2008a), "Electro-mechanical impedance based wireless structural health monitoring using PCA and k-means clustering algorithm",

Journal of Intelligent Materials Systems Structures, **19(**4), 509-520.

Park, G., Sohn, H., Farrar, C. R. and Inman, D. J. (2003), "Overview of piezoelectric impedance-based health monitoring and path forward", *The Shock and Vibration Digest*, **35**(5), 451-463.

Park, S., Yun, C. - B. and Inman, D. J. (2006), "Wireless structural health monitoring using an active sensing node", *Int. J. Steel Struct.*, **6**, 361–368.

Park, S., Yun, C. - B. and Inman, D. J. (2008b), "Structural health monitoring using electro-mechanical impedance sensors", *Fatigue & Fracture of Engineering Materials & Structures*, **31**, 714–724.

Shin, S.W., Qureshi, A.R., Lee, J.Y. and Yun, C.B. (2008), "Piezoelectric sensor based nondestructive active monitoring of strength gain in concrete," *Smart Materials and Structures*, **17**, 055002.

Soh, C. K., Tseng, K. K. H., Bhalla, S. and Gupta, A. (2000), "Performance of smart piezoceramic patches in health monitoring of a RC bridge", *Smart Materials and Structures*, **9**(4), 533-542.

Yang, Y., Lim, Y. Y. and Soh, C. K. (2008), "Practical issues related to the application of the

electromechanical impedance technique in the structural health monitoring of civil structures: I. Experiment", *Smart Materials and Structures*, **17**, 035008.

Yang, Y. and Miao, A. (2010) "Two-dimensional modeling of the effects of external vibration on the PZT impedance signature", *Smart Materials and Structures*, **19**, 065031.

Yun , C. – B. and Min, J. (2010), "Smart sensing, monitoring, and damage detection for civil infrastructures", *KSCE Journal of Civil Engineering*, **15**(1), 1-14.

Table 1: Configurations of aluminium beam specimens (231mm x 26mm x 4mm).

Specimens' labels	Location of PZT patch	Nature of Damage Induced	Stress Induced
T1	One-quarter from one end	Single edge crack	Tensile (constant)
C1	One-quarter from one end	Single edge crack	Compression (varying)
C2	Center	Bolt loosening	Compression (varying)

Table 2: Different levels of damages induced on specimen C2 through loosening of bolts.

Damage levels	**No. of bolts loosened**	**Descriptions**
0	0	Healthy (All bolts tightened)
1	1	Bolt C loosened
2	2	Bolt B & C loosened
3	3	Bolt A, B & C loosened
4	--	All bolts removed

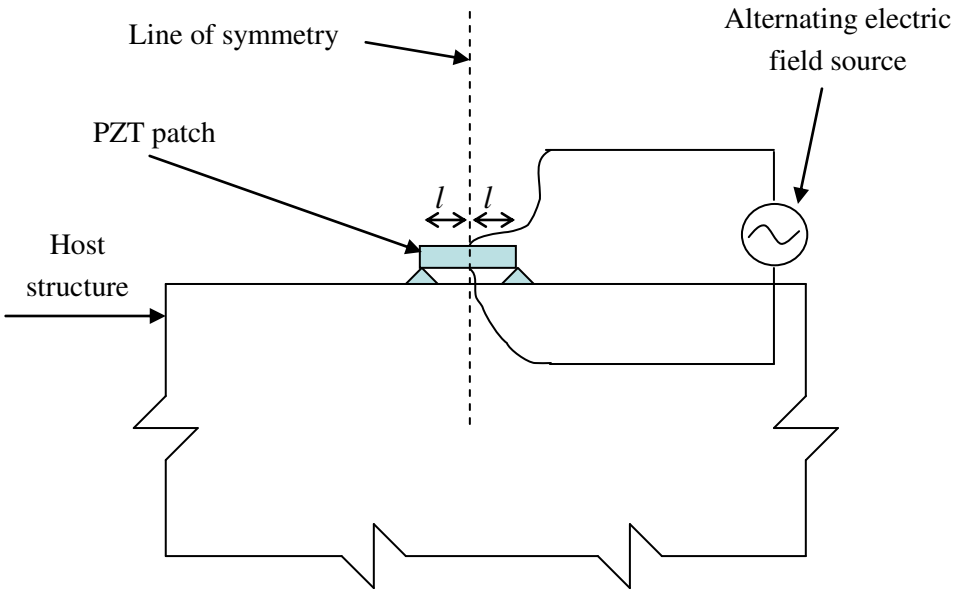

Fig. 1. Idealized interactions between a PZT patch and the host structure.

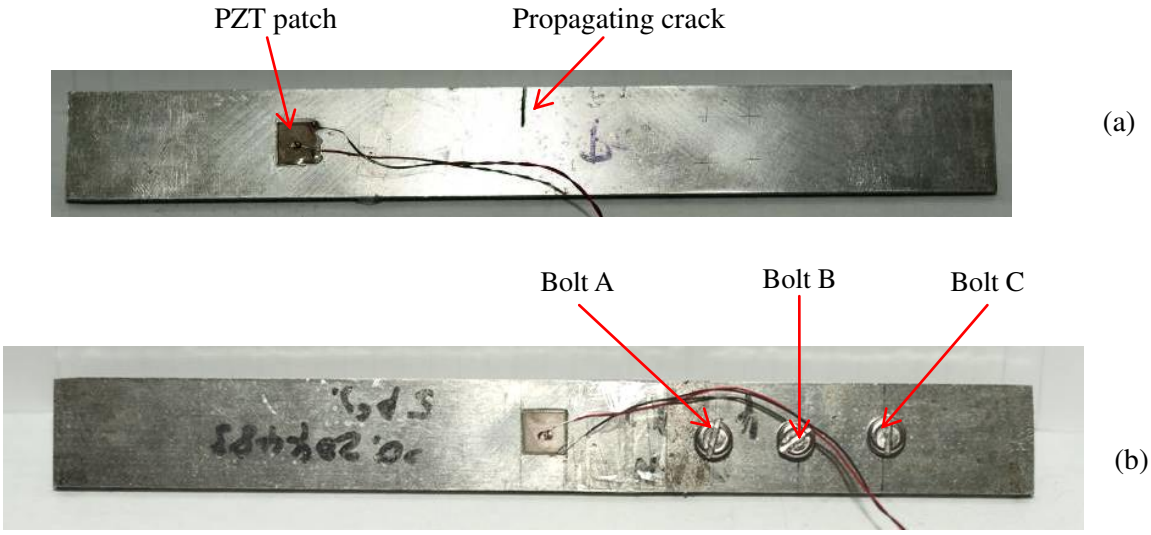

Fig. 2: Aluminum beam specimens (231mm x 26mm x 4mm) of different configurations.

(a) Specimen (T1 or C1)

(b) Specimen (C2)

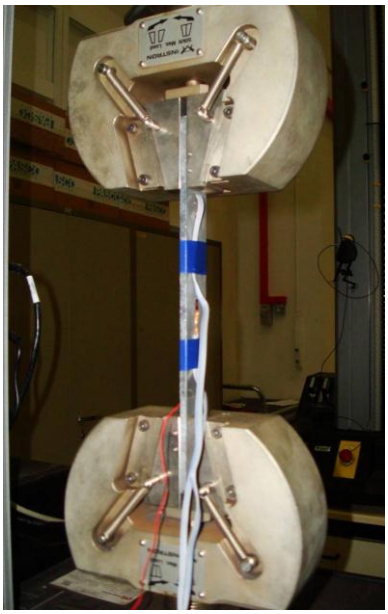

(a)

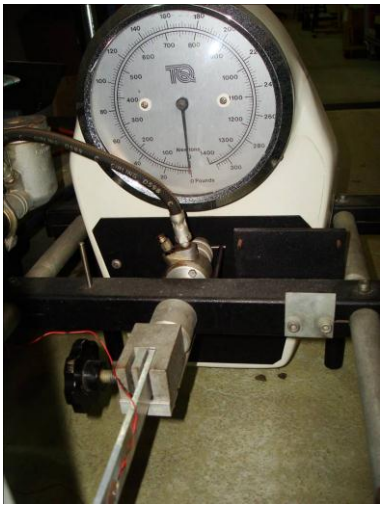

(b)

(c)

Fig. 3: Pictorial illustrations of experimental setup.

(a) UTM (b) Compressive strut rig (c) Precision impedance analyzer.

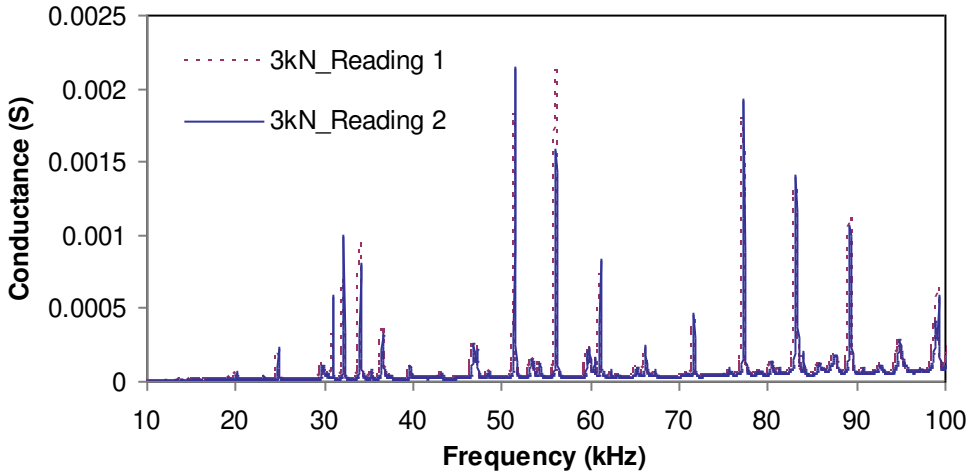

(a)

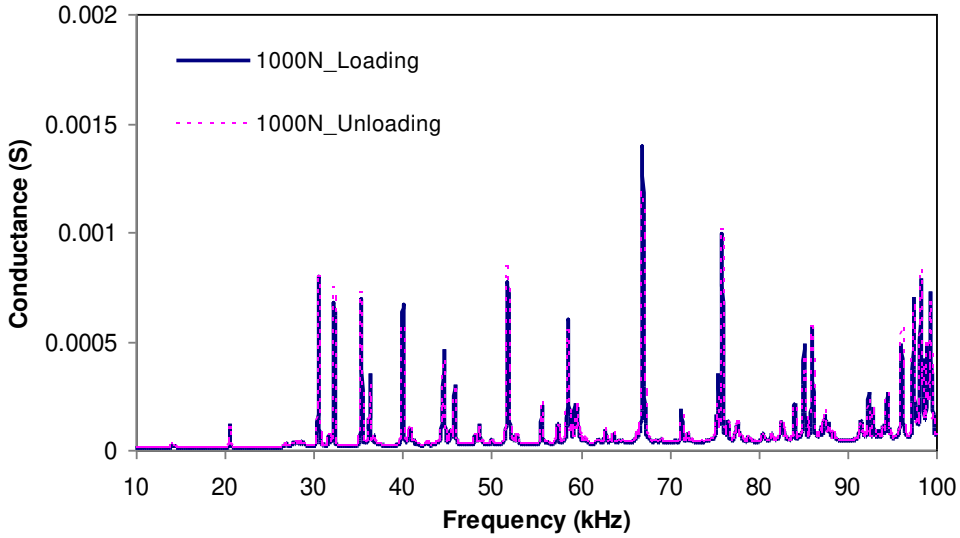

(b)

Fig. 4: Plot of conductance signatures versus frequency acquired from PZT patch surface-bonded on aluminium beam.

(a) Specimen T1 under 3kN of constant tensile load

(b) Specimen C1 under 1kN of compressive load (loading and unloading)

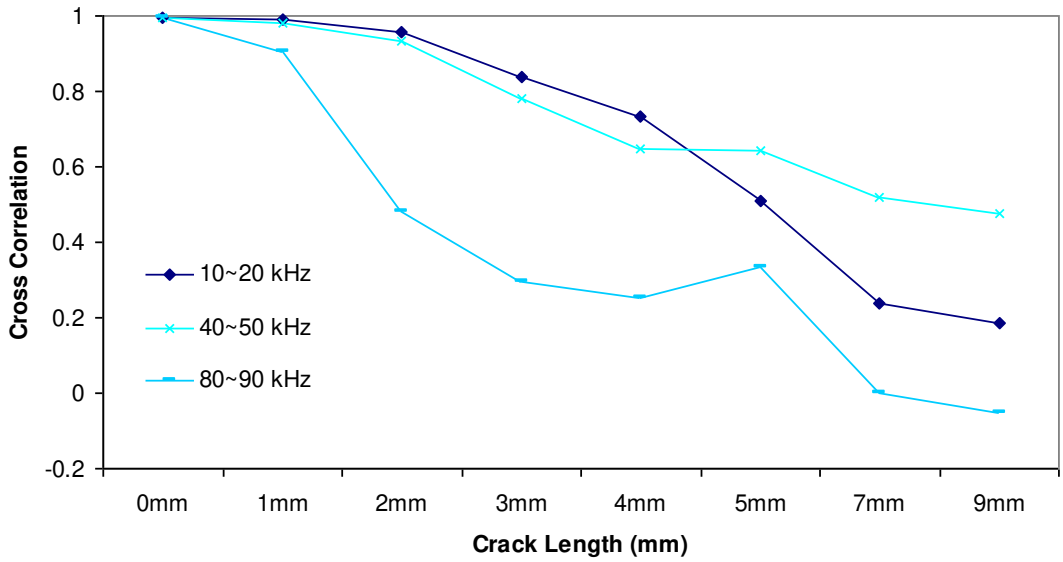

Fig. 5: Plot of CC indices evaluated from different frequency ranges versus crack length of specimen T1.

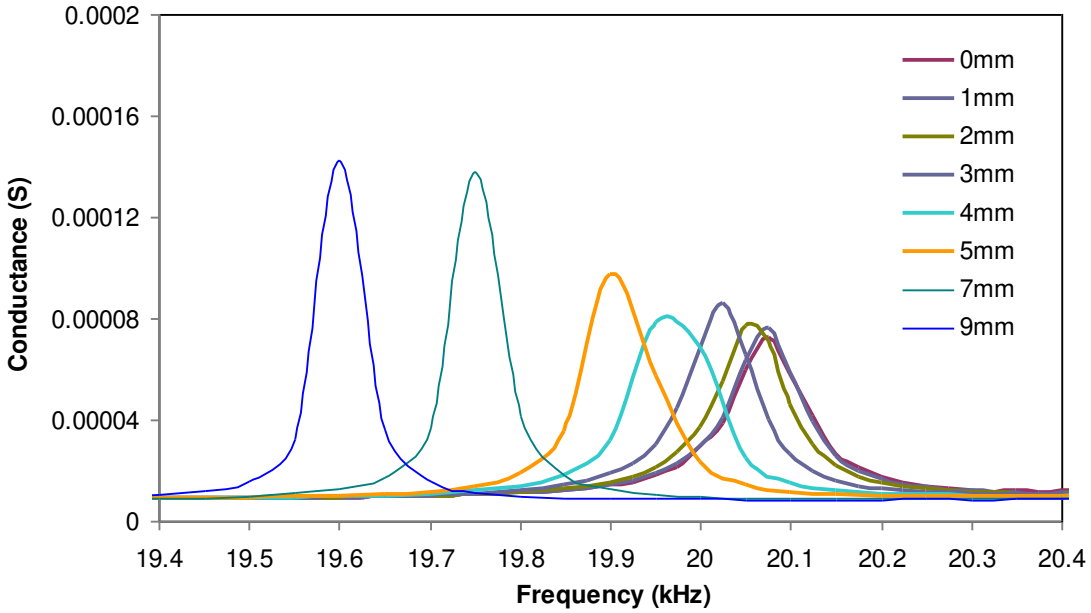

(a)

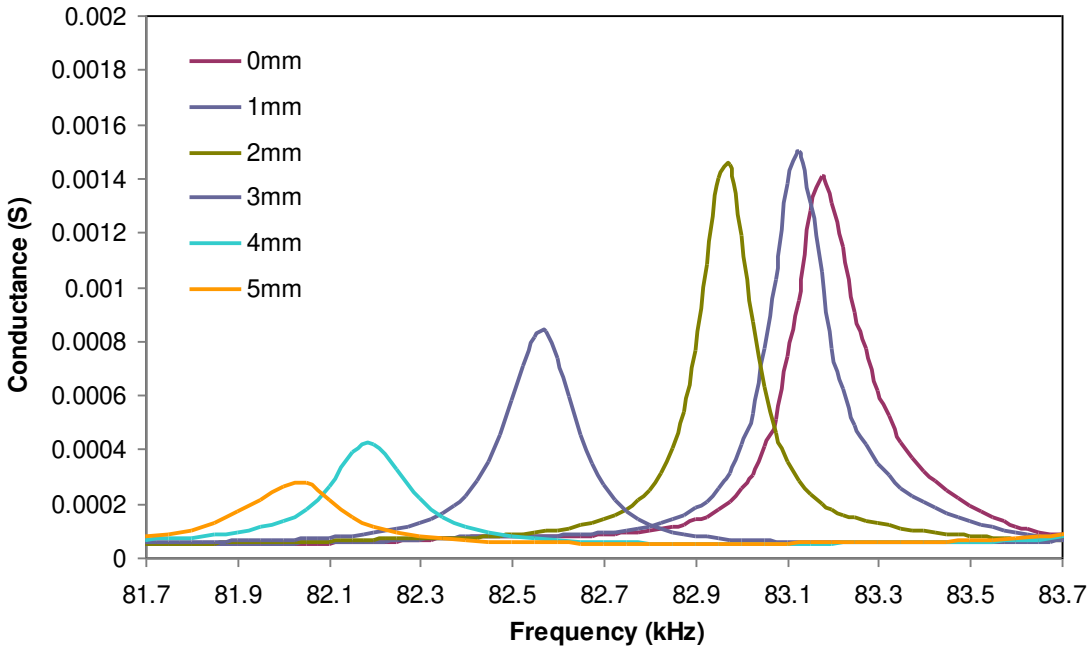

(b)

Fig. 6: Plot of conductance signatures versus frequency acquired from PZT patch surface-bonded on specimen T1 subjected to 3kN tensile force at various crack length.

(a) 19.4 ~ 20.4 kHz

(b) 81.7 ~ 83.7 kHz

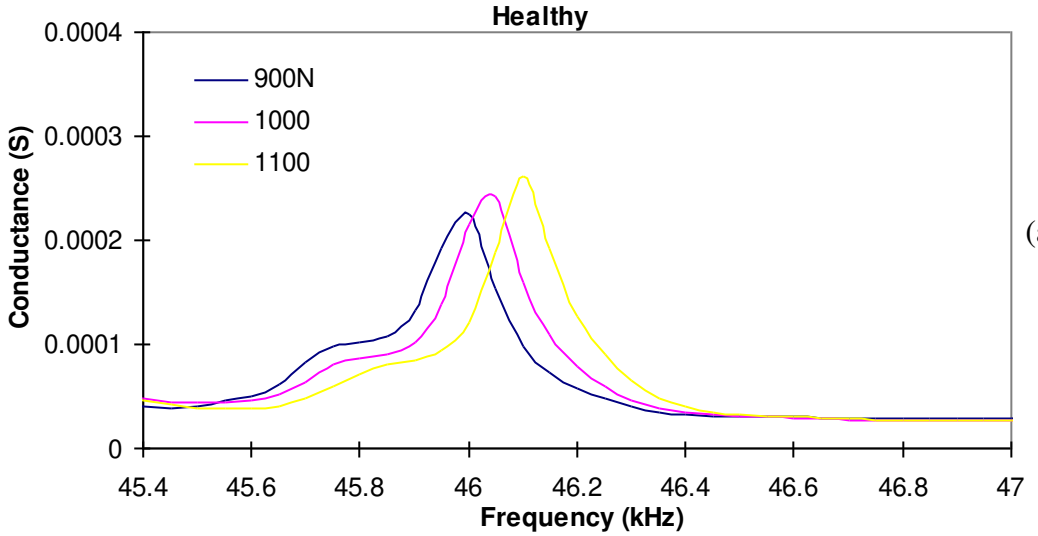

(a)

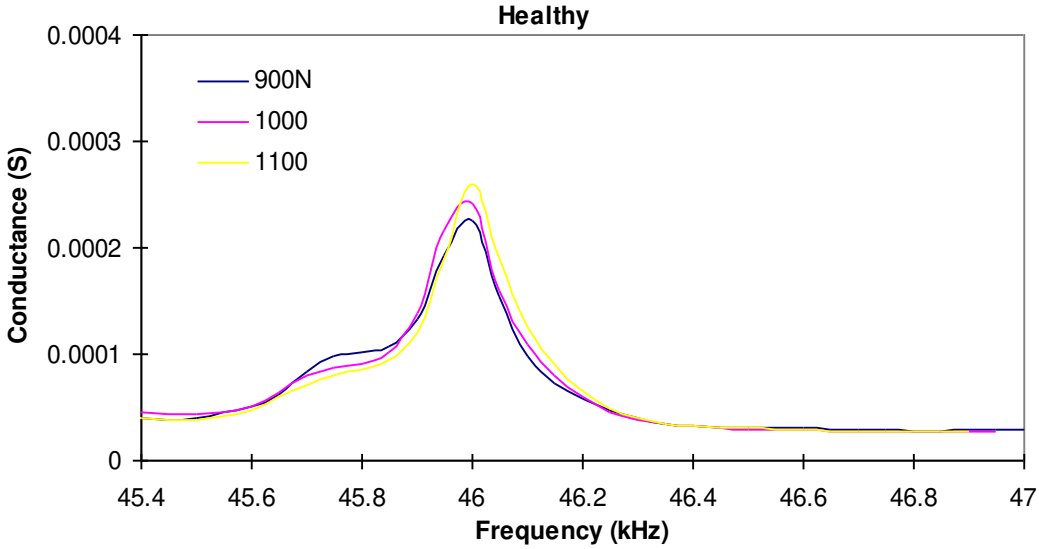

(b)

Fig. 7: Plot of conductance signatures versus frequency (45.4 ~ 47 kHz) acquired from specimen C1 under varying compressive load at healthy state.

(a) Before compensation

(b) After compensation

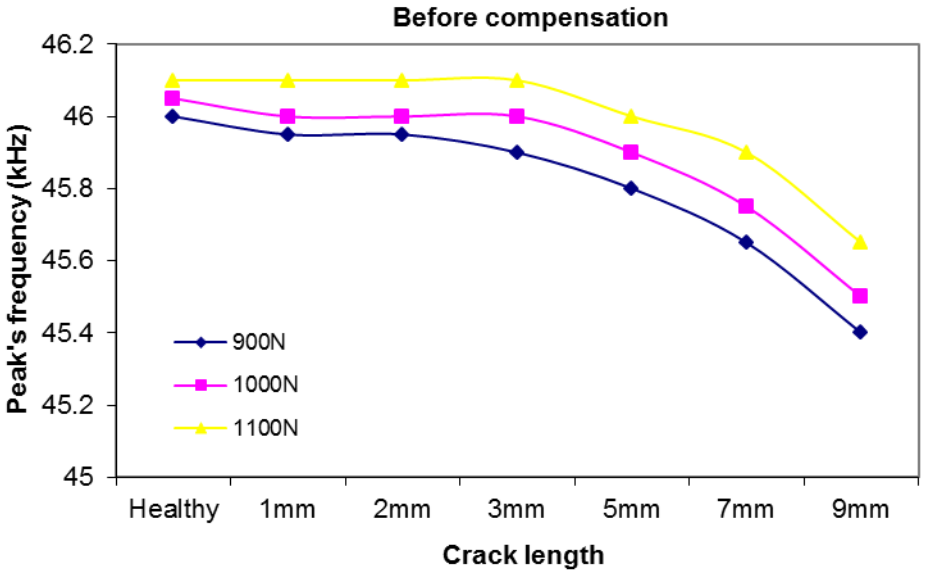
Before compensation
Peak's frequency (kHz)
46.2
46
45.8
45.6
45.4
45.2
45
900N
1000N
1100N
Healthy
1mm
2mm
3mm
5mm
7mm
9mm
Crack length

(a)

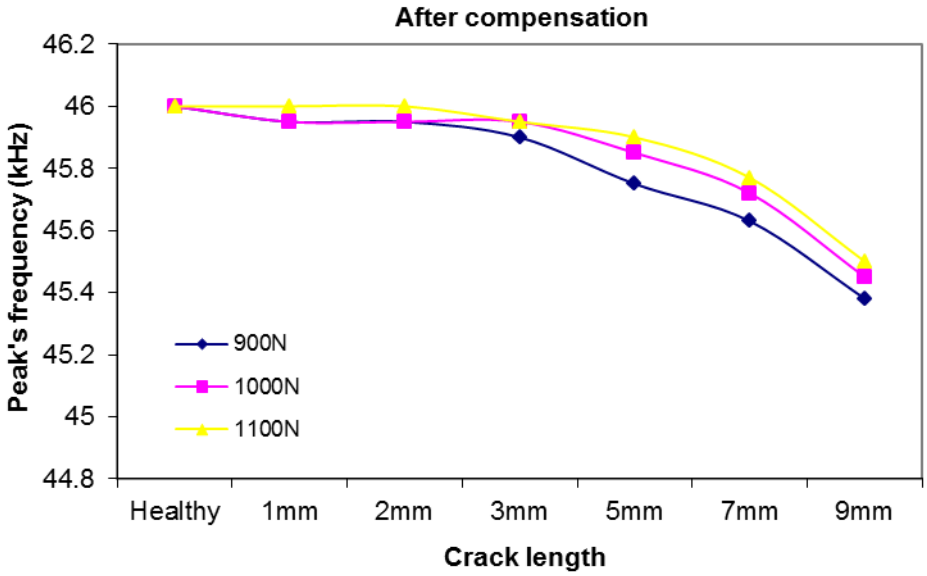
After compensation
Peak's frequency (kHz)
46.2
46
45.8
45.6
45.4
45.2
45
44.8
900N
1000N
1100N
Healthy
1mm
2mm
3mm
5mm
7mm
9mm
Crack length

(b)

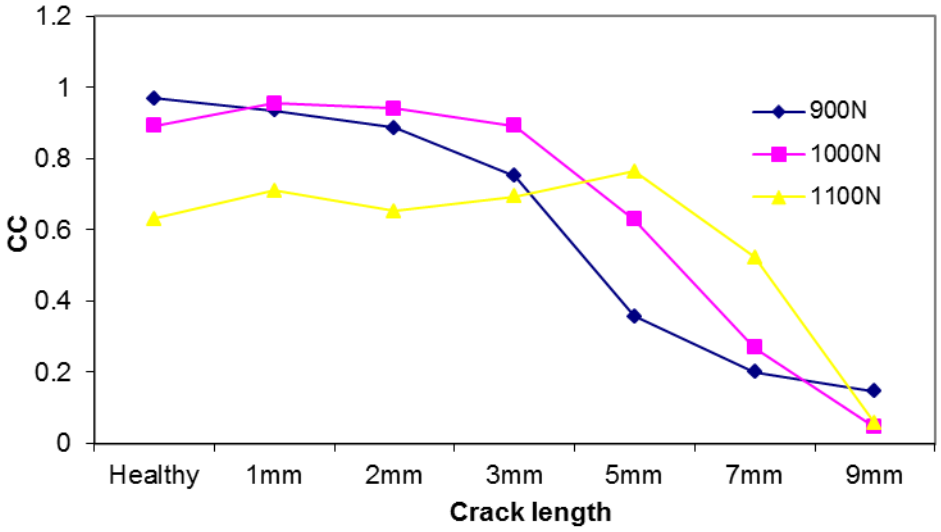

(c)

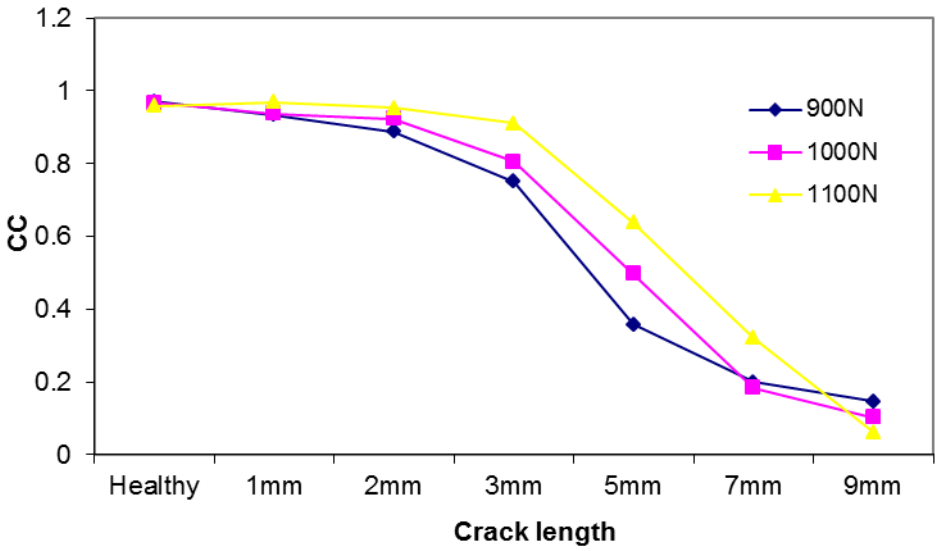

(d)

Fig. 8: Plot of peaks frequency and CC indices versus crack length of specimen C1 under varying compressive load.

(a) Peaks frequency (before compensation)

(b) Peaks frequency (after compensation)

(c) CC values from 44 ~ 47 kHz (before compensation)

(d) CC values from 44 ~ 47 kHz (after compensation)

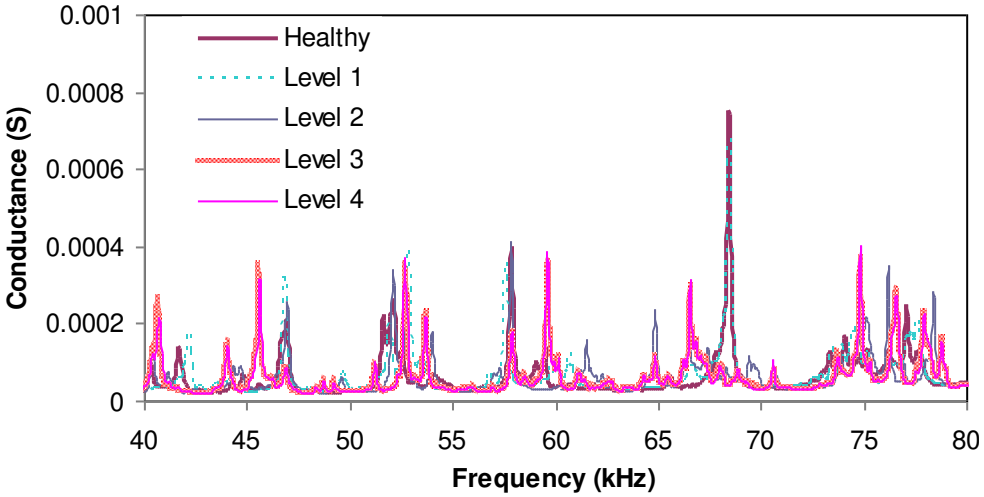

Fig. 9: Plot of conductance signatures versus frequency (40 ~ 80 kHz) acquired experimentally from PZT patch surface-bonded on specimen C2 at different damage levels under 900N compressive load.

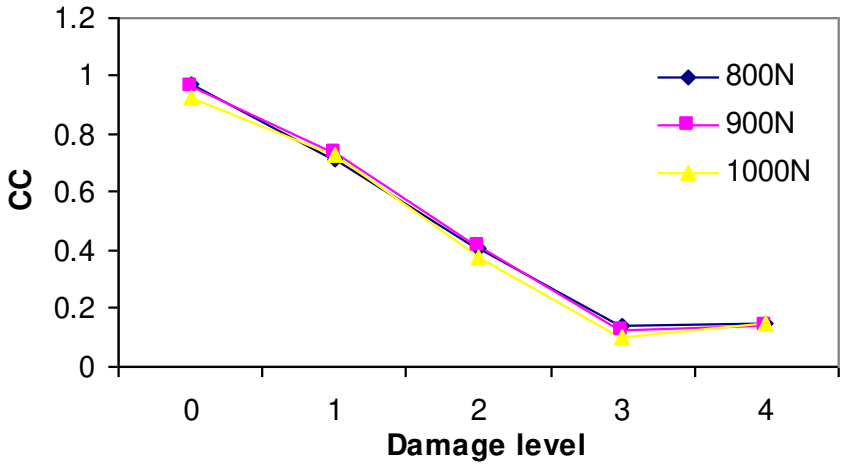

Fig. 10: CC index evaluated from conductance signatures (40 ~ 80 kHz) acquired from PZT patch surface-bonded on specimen C2 at different damage levels.